

# Trinuclear Copper(I) and Silver(I) Adducts of 4-Chloro-3,5-bis(trifluoromethyl)pyrazolate and 4-Bromo-3,5-bis(trifluoromethyl)pyrazolate

Champika V. Hettiarachchi,<sup>\*,†</sup> Manal A. Rawashdeh-Omary,<sup>\*,‡</sup> Daniel Korir,<sup>‡</sup> Jehan Kohistani,<sup>‡</sup> Muhammed Yousufuddin,<sup>§</sup> and H. V. Rasika Dias<sup>\*,§</sup>

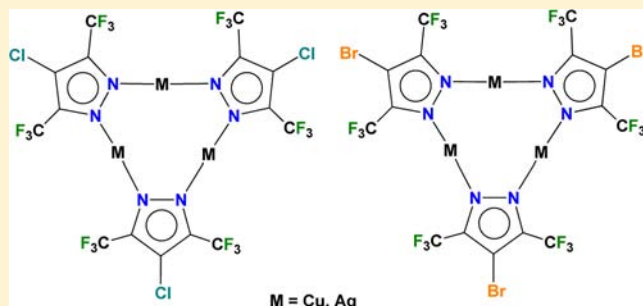
<sup>†</sup>Department of Chemistry, Faculty of Science, University of Peradeniya, Peradeniya 20400, Sri Lanka

<sup>‡</sup>Department of Chemistry and Physics, Texas Woman's University, Denton, Texas 76204, United States

<sup>§</sup>Department of Chemistry and Biochemistry, The University of Texas at Arlington, Arlington, Texas 76019, United States

## S Supporting Information

**ABSTRACT:** Syntheses, structural, and photoluminescence properties of  $\{[4\text{-X-3,5-(CF}_3)_2\text{Pz}]M\}_3$  ( $X = \text{Cl or Br, } M = \text{Cu or Ag}$ ) containing a heavier halide at the pyrazolyl ring 4-positions are reported. The  $\text{Cu}_2\text{O}$  and  $\text{Ag}_2\text{O}$  react with  $[4\text{-Cl-3,5-(CF}_3)_2\text{Pz}]H$  or  $[4\text{-Br-3,5-(CF}_3)_2\text{Pz}]H$  to form the corresponding metal pyrazolates, which are trinuclear adducts of the type  $\{[4\text{-X-3,5-(CF}_3)_2\text{Pz}]M\}_3$  with a nine-membered  $M_3N_6$  metallacyclic core. They also feature relatively short  $M\cdots\text{Cl}$  or  $M\cdots\text{Br}$  intertrimer separations ( $\sim 3.6 \text{ \AA}$ ) leading to supramolecular aggregates in the solid state. Distinct from the 4-H analogues  $\{[3,5\text{-(CF}_3)_2\text{Pz}]M\}_3$ , none of the four complexes described herein exhibits short intertrimer metal–metal interactions (as closest such  $M\cdots M$  separations are at a distance greater than  $5.0 \text{ \AA}$ ). The  $\{[4\text{-X-3,5-(CF}_3)_2\text{Pz}]M\}_3$  adducts exhibit bright photoluminescence even at room temperature. The photophysical data suggest that the  $\{[4\text{-X-3,5-(CF}_3)_2\text{Pz}]Cu\}_3$  complexes emit from an associative excited state, and the drastic Stokes shift suggests a significant change to the ground state structure of the trinuclear moiety and/or intermolecular interactions upon photoexcitation. The  $\{[4\text{-X-3,5-(CF}_3)_2\text{Pz}]Ag\}_3$  complexes emit from a ligand-centered excited state affected by silver and the heavier halogens. Thin films of  $\{[4\text{-X-3,5-(CF}_3)_2\text{Pz}]Cu\}_3$  trimers are promising for volatile organic compound (VOC) sensor applications as they exhibit luminescence color change upon exposure to vapors of benzene and its alkylated derivatives.



## INTRODUCTION

Homoleptic group 11 metal (i.e., copper, silver and gold) pyrazolates display a variety of solid state structures that range from trimers, tetramers, hexamers, to polymers.<sup>1–4</sup> Some of them also show interesting photophysical properties,<sup>5–12</sup> metallophilic bonding,<sup>4,6–9,15–19</sup>  $\pi$ -acid/ $\pi$ -base chemistry or  $\pi$ -acid/ $\sigma$ -donor interactions,<sup>12,14,17,20–26</sup> and dissociation-aggregation behavior in solution.<sup>15,27,28</sup> An area of major research focus in our laboratory has been the chemistry of fluorinated pyrazolyl and other azolyl ligands such as  $[3,5\text{-(CF}_3)_2\text{Pz}]^-$  (3,5-bis(trifluoromethyl)pyrazolate) and their coinage metal complexes.<sup>8,14,17,27,29–38</sup> For instance, we reported a convenient synthetic route to copper(I) and silver(I) adducts  $\{[3,5\text{-(CF}_3)_2\text{Pz}]Cu\}_3$  (**1**) and  $\{[3,5\text{-(CF}_3)_2\text{Pz}]Ag\}_3$  (**2**) using  $[3,5\text{-(CF}_3)_2\text{Pz}]H$  and the corresponding metal(I) oxides (Figure 1).<sup>14,29</sup> We have also reported remarkable photophysical properties and donor–acceptor chemistry of these trinuclear d<sup>10</sup> pyrazolates and that of the related  $\{[3,5\text{-(CF}_3)_2\text{Pz}]Au\}_3$ .<sup>8,14,17,30,35–37</sup> The copper adduct  $\{[3,5\text{-(CF}_3)_2\text{Pz}]Cu\}_3$  shows bright luminescence upon exposure to UV radiation, and the emission colors of solids and frozen-solutions display

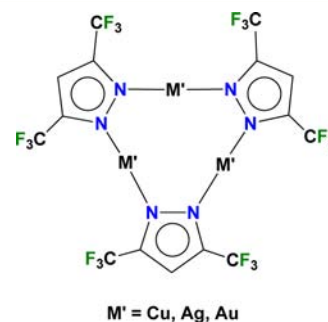


**Figure 1.** Copper(I), silver(I), and gold(I) complexes of  $[3,5\text{-(CF}_3)_2\text{Pz}]^-$ .

dramatic sensitivities to temperature, solvent, concentration, and excitation wavelengths.<sup>8,30</sup>  $\{[3,5\text{-(CF}_3)_2\text{Pz}]Ag\}_3$  is a strong  $\pi$ -acid and shows interesting chemistry with  $\pi$ -bases like benzene, toluene, mesitylene, and naphthalene.<sup>14,17,35–37</sup> The

Received: August 13, 2013

Published: November 8, 2013

photophysical properties associated with such  $\pi$ -acid/base interactions have included sensitive/selective vapochromic sensing of volatile organic compounds (VOCs), in particular benzene and its alkylated derivatives, as well as strong sensitization of the triplet state of naphthalene and other polynuclear aromatic hydrocarbons.<sup>36,37</sup> Other groups have also used these molecules for various purposes such as to examine excited state structures and as chemical vapor deposition (CVD) precursors.<sup>20,24,39,40</sup>

Changing the substituents on supporting ligands or even the supporting ligand itself is a convenient way to fine-tune the chemical and physical properties of these metal adducts. For example, studies indicate that  $\{[3,5-(\text{CF}_3)_2\text{Pz}]\text{Au}\}_3$  is a  $\pi$ -acid while  $\{[3,5-(\text{CH}_3)_2\text{Pz}]\text{Au}\}_3$  is a  $\pi$ -base.<sup>14,41</sup> Coinage metal adducts of sterically less demanding fluorinated pyrazolyl ligands like  $[3-(\text{CF}_3)\text{Pz}]^-$  or bulkier  $[3-(\text{C}_3\text{F}_7),5-(\text{Bu}^t)\text{Pz}]^-$  systems (relative to  $[3,5-(\text{CF}_3)_2\text{Pz}]^-$ ) have also been reported.<sup>17</sup> In this paper, we describe the synthesis, structures, and photophysical properties of hydrogen-free copper(I) and silver(I) adducts derived from pyrazolates bearing chloro and bromo substituents on the  $[3,5-(\text{CF}_3)_2\text{Pz}]^-$  ligand backbone (Figure 2). Although steric effects of  $[4\text{-Cl-}3,5-(\text{CF}_3)_2\text{Pz}]^-$  and

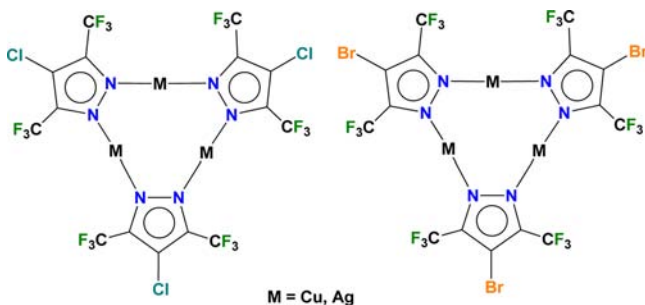


**Figure 2.** Copper(I) and silver(I) adducts of  $[4\text{-Cl-}3,5-(\text{CF}_3)_2\text{Pz}]^-$  and  $[4\text{-Br-}3,5-(\text{CF}_3)_2\text{Pz}]^-$ .

$[4\text{-Br-}3,5-(\text{CF}_3)_2\text{Pz}]^-$  ligands on a metal ion may not be very different from that of  $[3,5-(\text{CF}_3)_2\text{Pz}]^-$ , based on the  $\text{pK}_a$  values of  $[4\text{-Cl-}3,5-(\text{CF}_3)_2\text{Pz}]\text{H}$  (5.49),  $[4\text{-Br-}3,5-(\text{CF}_3)_2\text{Pz}]\text{H}$  (6.02), and  $[3,5-(\text{CF}_3)_2\text{Pz}]\text{H}$  (7.10),<sup>42</sup> the pyrazolates derived from two former pyrazoles should be electronically different and are expected to have less nucleophilic nitrogen sites. Thus, they may afford coinage metal adducts with even more  $\pi$ -acidic properties than  $\{[3,5-(\text{CF}_3)_2\text{Pz}]\text{Cu}\}_3$  (1) and  $\{[3,5-(\text{CF}_3)_2\text{Pz}]\text{Ag}\}_3$  (2).

## RESULTS AND DISCUSSION

**Synthesis and X-ray Crystal Structures.** Convenient routes to the two precursor pyrazoles  $[4\text{-Cl-}3,5-(\text{CF}_3)_2\text{Pz}]\text{H}$  and  $[4\text{-Br-}3,5-(\text{CF}_3)_2\text{Pz}]\text{H}$  containing chloro and bromo groups, respectively, at the fourth position of the pyrazole ring of  $[3,5-(\text{CF}_3)_2\text{Pz}]\text{H}$  have been reported by Maspero and co-workers.<sup>42</sup> The copper(I) and silver(I) pyrazolates  $\{[4\text{-Cl-}3,5-(\text{CF}_3)_2\text{Pz}]\text{Cu}\}_3$  (3),  $\{[4\text{-Br-}3,5-(\text{CF}_3)_2\text{Pz}]\text{Cu}\}_3$  (4),  $\{[4\text{-Cl-}3,5-(\text{CF}_3)_2\text{Pz}]\text{Ag}\}_3$  (5), and  $\{[4\text{-Br-}3,5-(\text{CF}_3)_2\text{Pz}]\text{Ag}\}_3$  (6) can be synthesized quite easily by treating metal(I) oxides  $\text{Cu}_2\text{O}$  and  $\text{Ag}_2\text{O}$  with the corresponding pyrazoles  $[4\text{-Cl-}3,5-(\text{CF}_3)_2\text{Pz}]\text{H}$  or  $[4\text{-Br-}3,5-(\text{CF}_3)_2\text{Pz}]\text{H}$  in about 1:2 molar ratio in benzene or toluene containing a few drops of acetonitrile. Compounds  $\{[4\text{-X-}3,5-(\text{CF}_3)_2\text{Pz}]\text{M}\}_3$  (X = Cl or Br, M = Cu or Ag) were obtained as white crystalline solids. The <sup>19</sup>F or <sup>13</sup>C NMR chemical shift values of these metal

adducts do not show a significant difference compared to the corresponding values of the free ligands. Crystals of the silver adducts  $\{[4\text{-Cl-}3,5-(\text{CF}_3)_2\text{Pz}]\text{Ag}\}_3$  and  $\{[4\text{-Br-}3,5-(\text{CF}_3)_2\text{Pz}]\text{Ag}\}_3$  suitable for X-ray diffraction studies were grown at 5 °C from hexane and  $\text{CH}_2\text{Cl}_2$ , respectively, and the X-ray data were collected at 100 K. The copper adducts  $\{[4\text{-Cl-}3,5-(\text{CF}_3)_2\text{Pz}]\text{Cu}\}_3$  and  $\{[4\text{-Br-}3,5-(\text{CF}_3)_2\text{Pz}]\text{Cu}\}_3$  were recrystallized at the ambient temperature from hexane. Unfortunately these copper pyrazolate crystals tend to crack at 100 K and therefore the X-ray data were collected at room temperature (RT).

The molecular structure of  $\{[4\text{-Cl-}3,5-(\text{CF}_3)_2\text{Pz}]\text{Cu}\}_3$  is illustrated in Figure 3. It adopts a trinuclear structure with an

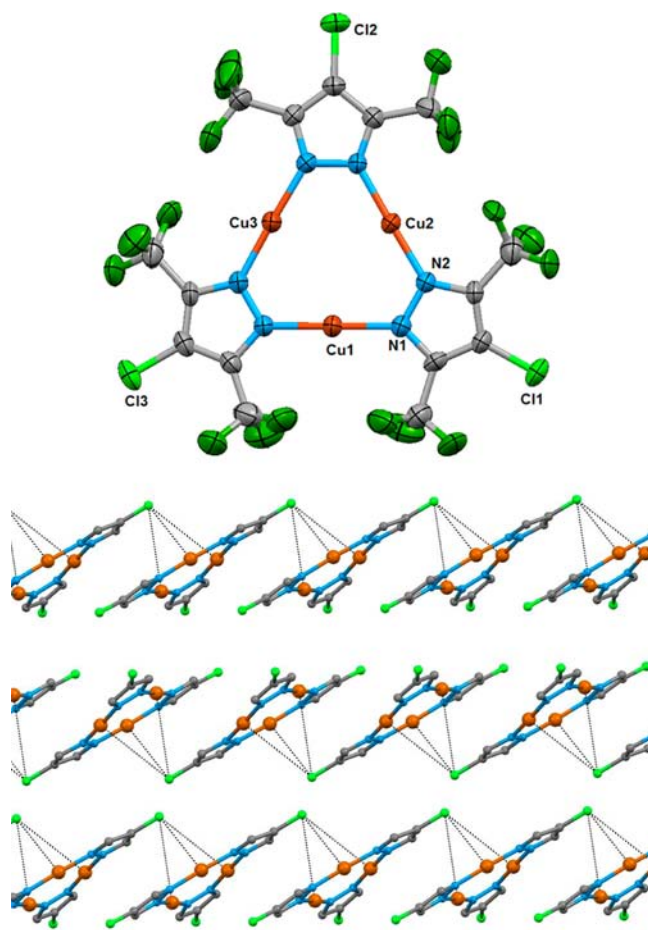


**Figure 3.** Molecular structure of  $\{[4\text{-Cl-}3,5-(\text{CF}_3)_2\text{Pz}]\text{Cu}\}_3$  and a view showing intertrimer  $\text{Cu}\cdots\text{Cl}$  separations leading to supra-molecular structure ( $\text{CF}_3$  groups have been omitted for clarity in the bottom figure).

essentially planar nine-membered  $\text{Cu}_3\text{N}_6$  metallacycle. Unlike  $\{[3,5-(\text{CF}_3)_2\text{Pz}]\text{Cu}\}_3$  which features zigzag chains with somewhat close intertrimer  $\text{Cu}\cdots\text{Cu}$  contacts (closest at 3.232 Å, Table 1),  $\{[4\text{-Cl-}3,5-(\text{CF}_3)_2\text{Pz}]\text{Cu}\}_3$  does not have intertrimer copper atoms at a close distance (closest intertrimer  $\text{Cu}\cdots\text{Cu}$  at 5.08 Å, which can be compared to Bondi's van der Waals contact separation of (two copper atoms of) 2.80 Å).<sup>43</sup> The closest intertrimer separations involving elements in the third period and higher (heavier atoms) are between Cu and Cl (closest of which is at 3.60 Å but they are longer than the sum of Bondi's van der Waals radii of copper and chlorine,  $1.40 + 1.75 = 3.15$  Å).<sup>43</sup> As shown in Figure 3, one chlorine atom of each of the trinuclear  $\{[4\text{-Cl-}3,5-(\text{CF}_3)_2\text{Pz}]\text{Cu}\}_3$  shows three

**Table 1. Selected Structural Parameters for {[4-Cl-3,5-(CF<sub>3</sub>)<sub>2</sub>Pz]Cu}<sub>3</sub> (3), {[4-Br-3,5-(CF<sub>3</sub>)<sub>2</sub>Pz]Ag}<sub>3</sub> (5), and {[4-Br-3,5-(CF<sub>3</sub>)<sub>2</sub>Pz]Ag}<sub>3</sub> (6) and the Related {[3,5-(CF<sub>3</sub>)<sub>2</sub>Pz]Cu}<sub>3</sub> (1) and {[3,5-(CF<sub>3</sub>)<sub>2</sub>Pz]Ag}<sub>3</sub> (2)**

parameters	1	2	3	4	5	6
M–N (range)/Å	1.855(2)–1.863(2)	1.864(3)–1.878(3)	1.862(4)–1.873(5)	1.864(3)–1.878(3)	2.098(4)–2.112(4)	2.102(3)–2.115(3)
N–M–N (range)/deg	178.4(1)–178.6(1)	176.8(2)–178.0(2)	177.2(2)–178.3(2)	176.8(2)–178.0(2)	177.7(2)–178.5(1)	176.8(1)–178.9(1)
closest M···M(intra M <sub>3</sub> )/Å	3.232	3.214	3.210	3.214	3.4968	3.443
closest M···M(inter M <sub>3</sub> )/Å	3.813	5.132	5.076	5.132	5.670	5.754
C–X (range)/Å		1.851(4)–1.866(4)	1.716(6)–1.719(6)	1.851(4)–1.866(4)	1.711(4)–1.719(4)	1.865(3)–1.876(4)
M···X(range) (intertrimer)/Å	14	3.555–4.129	3.604–4.637	3.555–4.129	3.658–4.159	3.568–3.916
ref		this work	this work		this work	this work

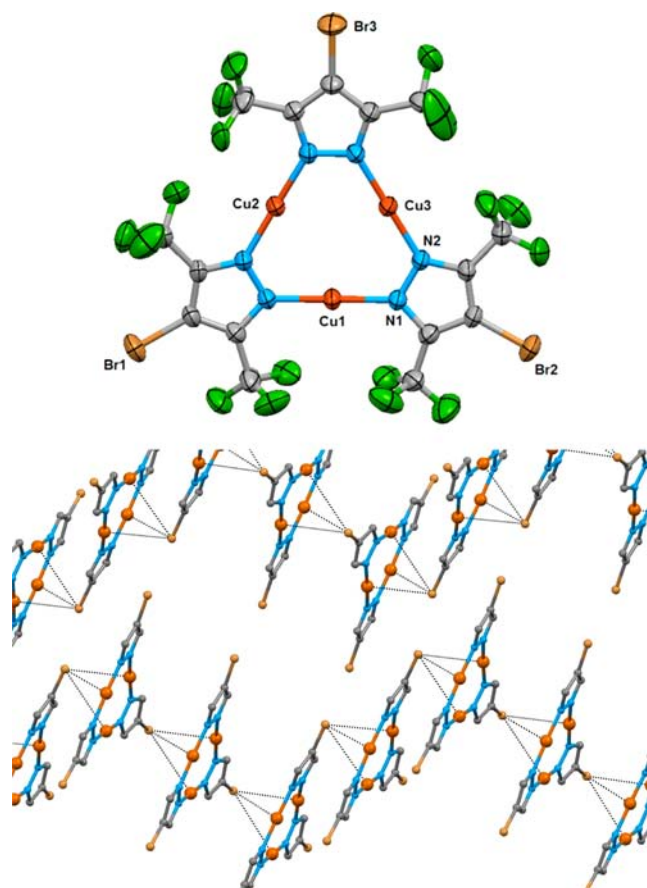


**Figure 4.** Molecular structure of {[4-Br-3,5-(CF<sub>3</sub>)<sub>2</sub>Pz]Cu}<sub>3</sub> and a view showing intertrimer Cu···Br arrangement leading to zigzag chains (CF<sub>3</sub> groups have been omitted for clarity in the bottom figure).

crystallographically distinct molecules of {[4-Br-3,5-(CF<sub>3</sub>)<sub>2</sub>Pz]Cu}<sub>3</sub> in the asymmetric unit. It also features a trinuclear structure in the solid state. Again, copper atoms of neighboring trimers are not close (closest Cu···Cu at 5.13 Å) and not directly above each other. Closest intertrimer heavier atom (elements in the third period and higher) separations are of the Cu···Br type with the closest approach at 3.55 Å. For comparison, the sum of the Bondi's van der Waals radii of copper and bromine is 1.40 + 1.85 = 3.25 Å.<sup>43</sup> There are three Cu···Br intertrimer separations in the range 3.55–4.13 Å between a bromine atom of each of the trimers and Cu<sub>3</sub> core of the neighboring trimers as depicted in Figure 4 so that it forms a distorted trigonal pyramidal structure with the Br atom at the

such Cu···Cl intertrimer separations at 3.60, 4.43, and 4.64 Å, so that it forms a distorted trigonal pyramid-like structure with the Cl atom at the vertex situated on one side of the nine-membered Cu<sub>3</sub>N<sub>6</sub> metallacyclic or the triangular Cu<sub>3</sub> core.<sup>44–46</sup> The other side of the Cu<sub>3</sub> core remains somewhat open, hence it is susceptible to interaction with guest molecules (vide infra). These Cu···Cl intertrimer alignments give rise to an extended stair-step structural motif in the {[4-Cl-3,5-(CF<sub>3</sub>)<sub>2</sub>Pz]Cu}<sub>3</sub> crystal. There are also several intermolecular C···F and F···F interactions between neighboring trimers. The Cu–N and intratrimer Cu···Cu distances are similar between {[3,5-(CF<sub>3</sub>)<sub>2</sub>Pz]Cu}<sub>3</sub> and {[4-Cl-3,5-(CF<sub>3</sub>)<sub>2</sub>Pz]Cu}<sub>3</sub> (see Table 1).

The molecular structure of {[4-Br-3,5-(CF<sub>3</sub>)<sub>2</sub>Pz]Cu}<sub>3</sub> is illustrated in Figure 4. There are two chemically similar but

vertex situated on one side of the triangular  $\text{Cu}_3$  core.<sup>44–46</sup> The other side of the  $\text{Cu}_3$  core remains somewhat open as observed for  $\{[4\text{-Cl-3,5-(CF}_3)_2\text{Pz]Cu}\}_3$ .

Overall, these  $\text{Cu}\cdots\text{Br}$  intertrimer contacts of  $\{[4\text{-Br-3,5-(CF}_3)_2\text{Pz]Cu}\}_3$  give rise to an extended stepladder structure but unlike in the  $\{[4\text{-Cl-3,5-(CF}_3)_2\text{Pz]Cu}\}_3$  crystal, the direction of the extended chain changes after three-repeating units because of the involvement of a Br atom pointed in a different direction. There are several intermolecular  $\text{C}\cdots\text{F}$  and  $\text{F}\cdots\text{F}$  interactions between neighboring trimers. A comparison of  $\text{Cu-N}$  and intratrimer  $\text{Cu}\cdots\text{Cu}$  distances of  $\{[3,5\text{-(CF}_3)_2\text{Pz]Cu}\}_3$ , and  $\{[4\text{-Cl-3,5-(CF}_3)_2\text{Pz]Cu}\}_3$  and  $\{[4\text{-Br-3,5-(CF}_3)_2\text{Pz]Cu}\}_3$  shows that there is no significant change in these parameters as a result of replacing hydrogen atoms at the pyrazolyl ring 4-position with chlorine or bromine atoms (see Table 1).

We have also investigated the solid state structures of the silver congeners. As depicted in Figures 5 and 6,  $\{[4\text{-Cl-3,5-}$

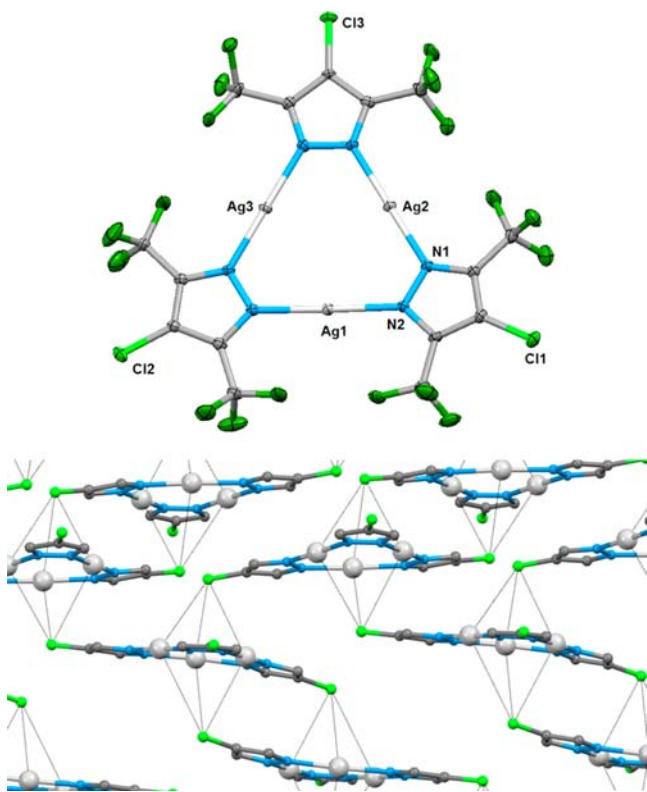


**Figure 5.** Molecular structure of  $\{[4\text{-Cl-3,5-(CF}_3)_2\text{Pz]Ag}\}_3$  and a view showing intertrimer  $\text{Ag}\cdots\text{Cl}$  contacts leading to aggregates ( $\text{CF}_3$  groups have been omitted for clarity in the bottom figure).

$(\text{CF}_3)_2\text{Pz]Ag}\}_3$  and  $\{[4\text{-Br-3,5-(CF}_3)_2\text{Pz]Ag}\}_3$  also adopt familiar trinuclear structures. Unlike  $\{[3,5\text{-(CF}_3)_2\text{Pz]Ag}\}_3$  which features short intertrimer  $\text{Ag}\cdots\text{Ag}$  contacts (3.2037 Å; Table 1), these 4-chloro and 4-bromo analogues do not form extended structures with close  $\text{Ag-Ag}$  separations (closest separations are at a distance of 5.67 and 5.75 Å, respectively, at an acute angle). Instead, these molecules form extended structures as illustrated in Figures 5 and 6 with somewhat close  $\text{Ag}\cdots\text{Cl}$  (closest at 3.66 Å with total six such separations in the range 3.66–4.16 Å) and  $\text{Ag}\cdots\text{Br}$  (closest at 3.57 Å with total six such separations in the range 3.57–3.92 Å) contacts. They are much closer to the Bondi's van der Waals contact distance of silver and chlorine ( $1.72 + 1.75 = 3.47$  Å) and silver and

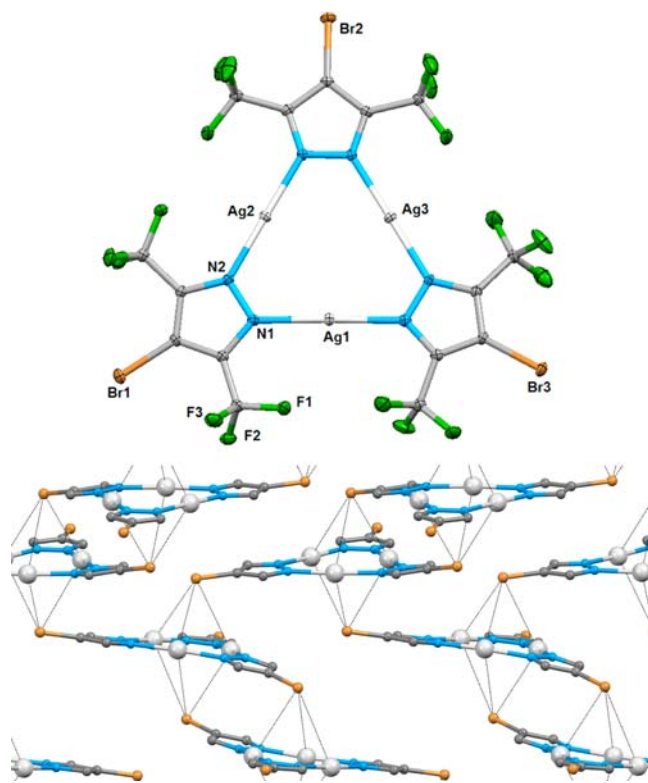


**Figure 6.** Molecular structure of  $\{[4\text{-Br-3,5-(CF}_3)_2\text{Pz]Ag}\}_3$  and a view showing intertrimer  $\text{Ag}\cdots\text{Br}$  placement leading to aggregates ( $\text{CF}_3$  groups have been omitted for clarity in the bottom figure).

bromine ( $1.72 + 1.85 = 3.57$  Å) than the related  $\text{Cu}\cdots\text{halide}$  separations relative to the corresponding  $\text{Cu-halide}$  van der Waals contact distance in the copper adducts.<sup>43–46</sup>

In contrast to the  $\{[4\text{-Cl-3,5-(CF}_3)_2\text{Pz]Cu}\}_3$ , two (not one) chlorine atoms of each  $\{[4\text{-Cl-3,5-(CF}_3)_2\text{Pz]Ag}\}_3$  show close intertrimer separations. Furthermore, each  $\text{Ag}_3$  core lies relatively close to two chlorine atoms of the neighboring trimers, so that it forms a distorted  $\text{Cl}_2\text{Ag}_3$  trigonal bipyramidal like structure with the Cl atom at the vertex situated on both sides of the nine-membered  $\text{Ag}_3\text{N}_6$  metallacycle. Overall, this arrangement leads to a 3D-network structure as illustrated in Figure 5 rather than chains. In addition, there are a number of intertrimer  $\text{C}\cdots\text{F}$ ,  $\text{N}\cdots\text{F}$ , and  $\text{F}\cdots\text{F}$  contacts. The 4-Br substituted analogue,  $\{[4\text{-Br-3,5-(CF}_3)_2\text{Pz]Ag}\}_3$ , also forms an extended structure similar to that observed for  $\{[4\text{-Cl-3,5-(CF}_3)_2\text{Pz]Ag}\}_3$ . It also has a  $\text{Ag}_3$  core sheltered from both top and bottom by a heavier halide.

It is interesting to compare the  $\text{Ag}\cdots\text{Br}$  contacts of  $\{[4\text{-Br-3,5-(CF}_3)_2\text{Pz]Ag}\}_3$  with other silver pyrazolates with similar contacts. The  $\{[4\text{-Br-3,5-(Ph)}_2\text{Pz]Ag}\}_3$  described by Raptis and co-workers features trigonal bipyramidal  $\text{Ag}_3\text{Br}_2$  motifs.<sup>23</sup> The  $\{[4\text{-Br-3,5-(i-Pr)}_2\text{Pz]Ag}\}_3$  also shows  $\text{Ag}\cdots\text{Br}$  contacts but contains distorted trigonal-pyramidal  $\text{Ag}_3\text{Br}$  motifs.<sup>33</sup> The  $\{[4\text{-Br-3,5-(i-Pr)}_2\text{Pz]Ag}\}_3$  exists as dimer-of-trimers with close  $\text{Ag}\cdots\text{Ag}$  contacts at 3.04 Å; thus the opposite  $\text{Ag}_3$  face is not accessible for  $\text{Ag}\cdots\text{Br}$  contacts. Furthermore, in both  $\{[4\text{-Br-3,5-(Ph)}_2\text{Pz]Ag}\}_3$  and  $\{[4\text{-Br-3,5-(i-Pr)}_2\text{Pz]Ag}\}_3$ , the bromine atoms are pointed toward the  $\text{Ag}_3$  core allowing relatively close  $\text{Ag-Br}$  approach with  $\text{Ag}\cdots\text{Br}$  contacts in the range 3.51–4.90 Å and 3.21–3.72 Å, respectively. The neighboring trimers of  $\{[4\text{-Br-3,5-(CF}_3)_2\text{Pz]Ag}\}_3$ , on the other hand, are essentially parallel to each other.

A comparison of Ag–N and intratrimer Ag⋯Ag distances of  $\{[3,5-(\text{CF}_3)_2\text{Pz}]\text{Ag}\}_3$ , and  $\{[4\text{-Cl-}3,5-(\text{CF}_3)_2\text{Pz}]\text{Ag}\}_3$  and  $\{[4\text{-Br-}3,5-(\text{CF}_3)_2\text{Pz}]\text{Ag}\}_3$  shows that there is no significant change in the Ag–N distances but the intratrimer Ag⋯Ag separations are smaller in the latter two species (see Table 1).

**Photoluminescence Data. Copper Complexes: Solid-State Luminescence Properties.** Considering the interesting photophysical properties displayed by  $\{[3,5-(\text{CF}_3)_2\text{Pz}]\text{Cu}\}_3$ , we have also investigated the solid-state luminescence properties of  $\{[4\text{-Cl-}3,5-(\text{CF}_3)_2\text{Pz}]\text{Cu}\}_3$  and  $\{[4\text{-Br-}3,5-(\text{CF}_3)_2\text{Pz}]\text{Cu}\}_3$ . Figure 7 and Supporting Information, Figure S1 show the

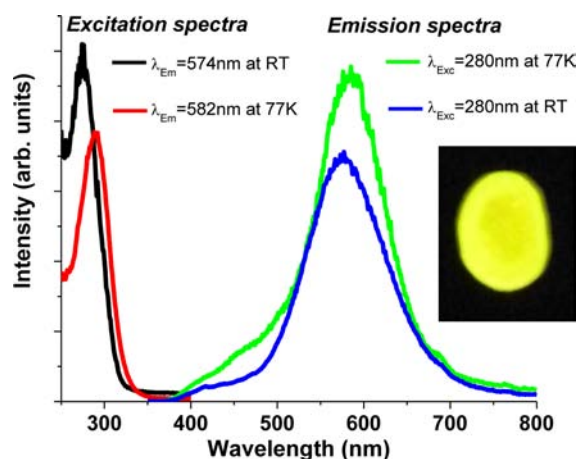


**Figure 7.** Emission and excitation spectra of a crystalline solid sample of  $\{[4\text{-Cl-}3,5-(\text{CF}_3)_2\text{Pz}]\text{Cu}\}_3$  at RT and 77 K. Inset: A photograph showing the emission color of solid  $\{[4\text{-Cl-}3,5-(\text{CF}_3)_2\text{Pz}]\text{Cu}\}_3$  sample at RT under UV irradiation.

photoluminescence emission and excitation spectra of crystalline solid samples of these adducts at RT and 77 K. Both compounds exhibit bright yellow emissions with maxima near 570–580 nm and very large Stokes shifts on the order of  $18,000\text{ cm}^{-1}$  ( $\lambda_{\text{exc}} \sim 260\text{--}280\text{ nm}$ ). For comparison,  $\{[3,5-(\text{CF}_3)_2\text{Pz}]\text{Cu}\}_3$  showed bright orange luminescence at RT and 77 K with emission maxima centered at 645 and 663 nm, respectively. Time-resolved data suggest phosphorescent excited states of triplet parentage with lifetimes in the 50–70  $\mu\text{s}$  range, which are rather similar to that obtained for the  $\{[3,5-(\text{CF}_3)_2\text{Pz}]\text{Cu}\}_3$  analogue.<sup>14</sup> The unstructured emission profile and large Stokes shift are suggestive of an intermolecular (associative) excited state behavior. An excited monomer-of-trimer molecule will likely exhibit a structured profile based on our previous experimental and theoretical investigations of this class of cyclic trinuclear complexes.<sup>14,34</sup> Charge transfer excited state admixtures have been proposed by Wang and co-workers for related polymeric structures that exhibit intramolecularly connected trinuclear copper(I) pyrazolates engaged in halide interactions.<sup>12</sup> The luminescence in those systems attained multiexponential lifetimes.<sup>12</sup> We exclude such mixed-state assignments given that we obtained monoexponential decays herein. Another intramolecularly connected trinuclear copper(I) pyrazolate system by Li and co-workers displayed multi-Gaussian peaks assigned to  $^*[\text{Cu}_3]_2$  excimers and  $^*[\text{Cu}_3]\cdots\text{I}$  exciplexes.<sup>26</sup> We again exclude such assignments because the systems herein exhibit a single emission band. The emission and excitation peaks exhibit subtle red and blue shifts, respectively, upon cooling to 77 K suggesting a greater degree of thermal contraction in the associative exciton than the

corresponding ground-state aggregate. In  $\{[3,5-(\text{CF}_3)_2\text{Pz}]\text{Cu}\}_3$ , the photoluminescence could be mainly attributed to metal centered emission modified by intertrimer  $\text{Cu}\cdots\text{Cu}$  cuprophilic interactions.<sup>8,14,40</sup> However, in  $\{[4\text{-Cl-}3,5-(\text{CF}_3)_2\text{Pz}]\text{Cu}\}_3$  and  $\{[4\text{-Br-}3,5-(\text{CF}_3)_2\text{Pz}]\text{Cu}\}_3$ , the intertrimer  $\text{Cu}\cdots\text{Cu}$  separations are rather long at 5.08 and 5.13 Å, respectively, and are significantly longer than Bondi's Cu–Cu van der Waals contact separation (2.80 Å)<sup>43</sup> to invoke a similar origin. We should, however, point out that these are ground state Cu⋯Cu separations, which are not necessarily the same in the excited state in which time-resolved crystallography may reveal drastic contractions.<sup>40</sup> Furthermore, recent reports by Butsanov and Alvarez place the van der Waals radius of copper at 2.0 and 2.38 Å (thus Cu–Cu van der Waals contact separation at 4.0 and 4.76 Å, respectively).<sup>44,45</sup> In addition, theoretical data suggest that interatomic attractive forces between two copper atoms extend even farther (i.e., they do not abruptly end at the van der Waals radii boundary).<sup>47,48</sup> Overall, the exact structural nature of the associative excited state is difficult to discern from the luminescence data alone and is in need of further investigations by methods such as time-resolved X-ray diffraction and computational modeling of the phosphorescent excited state, which we plan to pursue in the future.

**Copper Complexes: Thin-Film Luminescence Vapochromism.** Drop-cast thin films of  $\{[4\text{-Cl-}3,5-(\text{CF}_3)_2\text{Pz}]\text{Cu}\}_3$  and  $\{[4\text{-Br-}3,5-(\text{CF}_3)_2\text{Pz}]\text{Cu}\}_3$  showed similar emissions to those of the corresponding powders and single crystals; our previous work on the 4-H analogues substantiated such correlation based on comparison of the thin film powder diffraction. Films of both materials exhibit remarkable sensor potential upon VOC vapor exposure. Figure 8 and Supporting Information, Figure S2 show that introduction of vapors of benzene, toluene, or mesitylene to these thin films resulted in a dramatic color change of the photoluminescence, from yellow without vapor to green in the presence of vapor. The emission maxima are consistently blue-shifted in all experiments, from 580 nm for the dry films to  $\sim 560\text{ nm}$  for the vapor-exposed thin films. While benzene and toluene vapors resulted in significant luminescence vapochromic blue shift of both  $\{[4\text{-Cl-}3,5-(\text{CF}_3)_2\text{Pz}]\text{Cu}\}_3$  and  $\{[4\text{-Br-}3,5-(\text{CF}_3)_2\text{Pz}]\text{Cu}\}_3$  complexes, mesitylene vapor produced more significant quenching of the copper trimer emission.

The emission color/wavelength changes are fully reversible such that drying the vapor-exposed films via heat, vacuum, or air results in regeneration of the characteristic yellow emission of the dry film. The experiment was repeated for multiple vapor exposure-drying cycles and the same qualitative changes were reproduced. Control experiments with vapors of nonaromatic VOCs such as dichloromethane and acetone did not produce the color changes, suggesting the selectivity of the process. Overall, the luminescence vapochromic behavior of both these  $\{[4\text{-Cl-}3,5-(\text{CF}_3)_2\text{Pz}]\text{Cu}\}_3$  and  $\{[4\text{-Br-}3,5-(\text{CF}_3)_2\text{Pz}]\text{Cu}\}_3$  complexes is somewhat similar to our prior work on the silver(I) adduct  $\{[3,5-(\text{CF}_3)_2\text{Pz}]\text{Ag}\}_3$  in terms of selectivity to  $\pi$ -basic aromatic hydrocarbons and reversibility.<sup>37</sup> However, the sensing was on/off switching for  $\{[3,5-(\text{CF}_3)_2\text{Pz}]\text{Ag}\}_3$  as opposed to the emission color change herein.

**Silver Complexes: Solid-State Luminescence Properties.** Figure 9 and Supporting Information, Figure S3 show the photoluminescence emission and excitation spectra of crystalline solid samples of  $\{[4\text{-Cl-}3,5-(\text{CF}_3)_2\text{Pz}]\text{Ag}\}_3$  and  $\{[4\text{-Br-}3,5-(\text{CF}_3)_2\text{Pz}]\text{Ag}\}_3$  at RT and 77 K. Both compounds exhibit weak blue emissions with maxima near 450–480 nm that are tunable by temperature and varying the halide in the 4-position of the

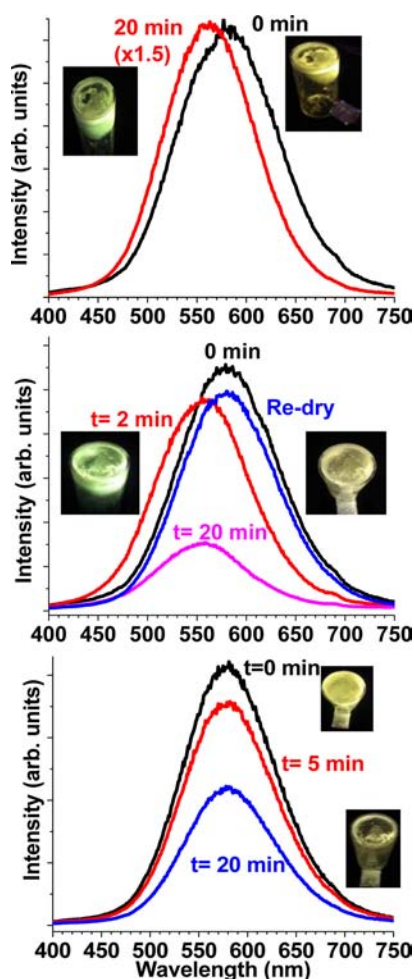


**Figure 8.** Photoluminescence spectral changes for a drop-cast thin film of {[4-Cl-3,5-(CF<sub>3</sub>)<sub>2</sub>Pz]Cu}<sub>3</sub> at RT (deposited from dichloromethane solution) upon introduction or removal of vapors of benzene (a; top), toluene (b; middle), or mesitylene (c; bottom).

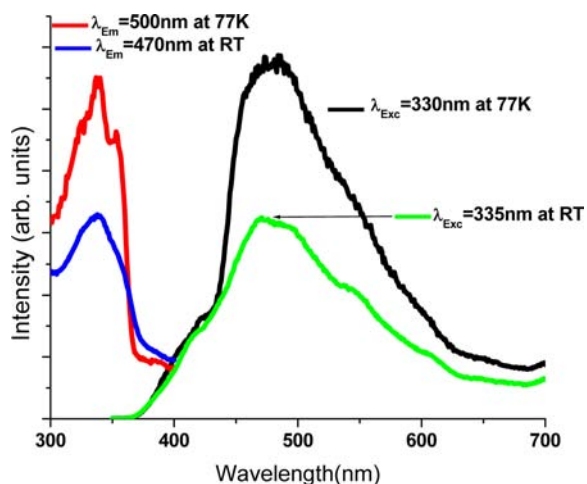


**Figure 9.** Photoluminescence emission and excitation spectra of a crystalline solid sample of {[4-Cl-3,5-(CF<sub>3</sub>)<sub>2</sub>Pz]Ag}<sub>3</sub> at RT and 77 K.

pyrazolate. Thus, fine-tuning of the blue emission wavelengths to 450, 465, 470, and 480 nm is attained upon changing the halide atom at the pyrazolyl ring 4-position and temperature. The emission bands are somewhat structured, although the resolution is not very high in view of signal weakness. Note that

{[3,5-(CF<sub>3</sub>)<sub>2</sub>Pz]Ag}<sub>3</sub> does not show photoluminescence at RT but emits light at 77 K (unstructured emission centered at 460 nm) upon UV excitation under similar conditions.<sup>14</sup>

An independent study of the luminescence of metal-free pyrazoles (the precursor pyrazoles used in this work) at 77 K (no luminescence at RT) reveals similar blue emission peaks in the same wavelength range and similar weakly resolved vibronic structure, as shown in Supporting Information, Figure S4. This suggests that the emission bands of silver complexes are ligand-centered emissions reflective of unassociated monomeric species. The Stokes shifts are less than 10,000 cm<sup>-1</sup> ( $\lambda_{\text{exc}} \sim 300\text{--}350\text{ nm}$ ), significantly smaller than those for the copper complexes, which also supports the ligand-centered assignment for the luminescence bands of the silver complexes. The fact that the emission maxima are blue-shifted while the excitation maxima are red-shifted for the silver complexes relative to the copper complexes is opposite to trends for the {[3,5-(CF<sub>3</sub>)<sub>2</sub>Pz]M'<sub>3</sub>} (M' = Cu, Ag, Au) complexes that exhibited metal-centered unstructured emission for all coinage metal species with relative energy that follows that for the free ion ( $\text{Au}^+ \sim \text{Cu}^+ \ll \text{Ag}^+$ ).<sup>14</sup> Time-resolved data suggest phosphorescent excited states of triplet parentage with lifetimes of  $\sim 7\ \mu\text{s}$  for both {[4-Cl-3,5-(CF<sub>3</sub>)<sub>2</sub>Pz]Ag}<sub>3</sub> and {[4-Br-3,5-(CF<sub>3</sub>)<sub>2</sub>Pz]Ag}<sub>3</sub> complexes at 77 K. Spin-orbit coupling of silver in combination with the heavy halide (Cl or Br) provides sufficient cooperative heavy-atom effect that is likely responsible for the observation of phosphorescence at RT for both silver complexes herein (Figure 9 and Supporting Information, Figure S3) but not the free ligand (Supporting Information, Figure S4) or the 4-H complex {[3,5-(CF<sub>3</sub>)<sub>2</sub>Pz]Ag}<sub>3</sub>, as the latter two solids only emit at 77 K. However, we should note that both {[4-Cl-3,5-(CF<sub>3</sub>)<sub>2</sub>Pz]Ag}<sub>3</sub> and {[4-Br-3,5-(CF<sub>3</sub>)<sub>2</sub>Pz]Ag}<sub>3</sub> samples slowly decompose under ambient conditions, which affect the emission intensity and energy with time.

**Silver Complexes: Thin-Film Luminescence Vapochromism.** Drop-cast thin films of silver adducts samples {[4-Cl-3,5-(CF<sub>3</sub>)<sub>2</sub>Pz]Ag}<sub>3</sub> and {[4-Br-3,5-(CF<sub>3</sub>)<sub>2</sub>Pz]Ag}<sub>3</sub> showed very weak to no luminescence, which is probably due to the instability of both complexes and/or air quenching. Neither film exhibits a promising sensor potential upon vapor exposure. A likely explanation is that Ag<sub>3</sub> centers of both {[4-Cl-3,5-(CF<sub>3</sub>)<sub>2</sub>Pz]Ag}<sub>3</sub> and {[4-Br-3,5-(CF<sub>3</sub>)<sub>2</sub>Pz]Ag}<sub>3</sub> are intermolecularly shielded by relatively closely positioned halogen atoms, as revealed by their X-ray structures, thus making them inaccessible to interaction with solvent molecules like arenes. This is in a stark contrast to the situation for the copper complexes {[4-Cl-3,5-(CF<sub>3</sub>)<sub>2</sub>Pz]Cu}<sub>3</sub> and {[4-Br-3,5-(CF<sub>3</sub>)<sub>2</sub>Pz]Cu}<sub>3</sub>, both of which exhibit an open face that is not engaged in intertrimer interactions with halogen atoms, thus allowing a significant sensing behavior to interact with the vapors of  $\pi$ -basic molecules.

## CONCLUSION

In summary, trinuclear copper(I) and silver(I) adducts {[4-X-3,5-(CF<sub>3</sub>)<sub>2</sub>Pz]M}<sub>3</sub> (X = Cl or Br and M = Cu or Ag) can be synthesized conveniently from the corresponding pyrazoles [4-X-3,5-(CF<sub>3</sub>)<sub>2</sub>Pz]H and the metal precursors, Cu<sub>2</sub>O or Ag<sub>2</sub>O. Distinct from the 4-H analogues {[3,5-(CF<sub>3</sub>)<sub>2</sub>Pz]M}<sub>3</sub>, the {[4-X-3,5-(CF<sub>3</sub>)<sub>2</sub>Pz]M}<sub>3</sub> complexes do not show intertrimer metal-metal interactions. Instead, they feature close intermolecular interactions involving M and Cl or Br ( $\sim 3.6\ \text{\AA}$ ) leading to supramolecular chains or network structures. Solid samples of {[4-X-3,5-(CF<sub>3</sub>)<sub>2</sub>Pz]M}<sub>3</sub> exhibit photoluminescence

both at RT and at 77 K. The M...M contacts are important for the luminescence of the analogous  $\{[3,5-(\text{CF}_3)_2\text{Pz}]\text{M}\}_3$  systems but in  $\{[4\text{-X-}3,5-(\text{CF}_3)_2\text{Pz}]\text{M}\}_3$  adducts, such separations are rather long, at least in the ground state.<sup>49</sup> Thin films of  $\{[4\text{-X-}3,5-(\text{CF}_3)_2\text{Pz}]\text{Cu}\}_3$  trimers are promising for VOC sensor applications as they both exhibit luminescence color change upon exposure to vapors of benzene and its alkylated derivatives. We are currently exploring the related gold chemistry, additional sensor applications, as well as the chemistry of mixed-metal systems.

## EXPERIMENTAL SECTION

**General Procedures.** All preparations and manipulations were carried out under nitrogen atmosphere using standard Schlenk technique. Commercially available solvents were purified and dried by standard methods and degassed twice by freeze–pump–thaw method prior to use. Glassware was oven-dried overnight at 150 °C. NMR spectra were acquired at 25 °C, on a JEOL Eclipse 500 spectrometer (<sup>19</sup>F, 470.62 MHz and <sup>13</sup>C, 125.77 MHz). <sup>19</sup>F NMR chemical shifts were referenced relative to external CFCl<sub>3</sub>. Melting points were obtained on a Mel-Temp II apparatus. Elemental analyses were performed using a Perkin-Elmer Model 2400 CHN analyzer. 4-Chloro-3,5-bis(trifluoromethyl)pyrazole, [4-Cl-3,5-(CF<sub>3</sub>)<sub>2</sub>Pz]H and 4-bromo-3,5-bis(trifluoromethyl)pyrazole [4-Br-3,5-(CF<sub>3</sub>)<sub>2</sub>Pz]H were prepared using procedures reported by Maspero et al.<sup>42</sup> Copper(I) oxide and silver(I) oxide were obtained from commercial sources and used as received. The details of the luminescence measurements, including instrumentation used in steady-state and time-resolved spectra, are discussed elsewhere.<sup>37</sup>

**Synthesis of  $\{[4\text{-Cl-}3,5-(\text{CF}_3)_2\text{Pz}]\text{Cu}\}_3$ .** A 30.0 mL portion of dry benzene was added to a mixture of Cu<sub>2</sub>O (0.145 g, 1.01 mmol) and [4-Cl-3,5-(CF<sub>3</sub>)<sub>2</sub>Pz]H (0.467 g, 1.96 mmol) in a Schlenk flask charged with N<sub>2</sub>. After adding 5 drops of acetonitrile, the mixture was refluxed overnight. After it was cooled to RT, the solution was filtered through a bed of Celite, and solvent was removed under reduced pressure to obtain an off white powder. It was then vacuum-dried at 80 °C for 5 h until there was no yellow photoluminescence upon 365 nm UV irradiation to obtain  $\{[4\text{-Cl-}3,5-(\text{CF}_3)_2\text{Pz}]\text{Cu}\}_3$ . Thin plate like crystals of  $\{[4\text{-Cl-}3,5-(\text{CF}_3)_2\text{Pz}]\text{Cu}\}_3$  suitable for X-ray data collection were grown at the ambient temperature from hexane. Yield: 89% (based on the amount of pyrazole used). Melting point 184–186 °C, <sup>19</sup>F NMR (CDCl<sub>3</sub>): δ -61.1 (s, CF<sub>3</sub>). <sup>13</sup>C NMR (CDCl<sub>3</sub>): δ 110.2 (s, 4-C), 119.4 (q, CF<sub>3</sub>, J<sub>C-F</sub> = 269.1 Hz), 141.5 (q, 3-C and 5-C, J<sub>C-F</sub> = 36.9 Hz). Anal. Calcd for C<sub>15</sub>Cu<sub>3</sub>N<sub>6</sub>F<sub>18</sub>Cl<sub>3</sub>: C, 19.95; H, 0.00; N, 9.30. Found: C, 19.96; H, <0.10, N, 10.72.

**Synthesis of  $\{[4\text{-Br-}3,5-(\text{CF}_3)_2\text{Pz}]\text{Cu}\}_3$ .** A 30.0 mL portion of dry benzene was added to a mixture of Cu<sub>2</sub>O (0.136 g, 0.95 mmol) and [4-Br-3,5-(CF<sub>3</sub>)<sub>2</sub>Pz]H (0.560 g, 1.93 mmol) in a Schlenk flask charged with N<sub>2</sub>. After adding 5 drops of acetonitrile, the mixture was refluxed overnight. After it was cooled, the solution was filtered through a bed of Celite, and solvent was removed under reduced pressure to obtain a white powder. It was vacuum-dried at 80 °C for 6 h until there was no yellow photoluminescence when irradiated at 365 nm to obtain  $\{[4\text{-Br-}3,5-(\text{CF}_3)_2\text{Pz}]\text{Cu}\}_3$ . The product was recrystallized from hexane at the ambient temperature to obtain thin plates. Yield: 91% (based on the amount of pyrazole used). Melting point 208–210 °C. <sup>19</sup>F NMR (CDCl<sub>3</sub>): δ -61.3 (s, CF<sub>3</sub>). <sup>13</sup>C NMR (CDCl<sub>3</sub>): δ 92.8 (s, 4-C), 119.5 (q, CF<sub>3</sub>, J<sub>C-F</sub> = 270.4 Hz), 143.5 (q, 3-C and 5-C, J<sub>C-F</sub> = 36.5 Hz). Anal. Calcd for C<sub>15</sub>Cu<sub>3</sub>N<sub>6</sub>F<sub>18</sub>Br<sub>3</sub>: C, 17.38; H, 0.00; N, 8.11. Found: C, 17.31; H, <0.10; N, 10.27 (Note: two different batches of sample were analyzed three separate times, but the observed %N was higher than expected, perhaps because of documented difficulties in complete combustion of some highly fluorinated samples).

**Synthesis of  $\{[4\text{-Cl-}3,5-(\text{CF}_3)_2\text{Pz}]\text{Ag}\}_3$ .** Ag<sub>2</sub>O (0.244 g, 1.05 mmol) and [4-Cl-3,5-(CF<sub>3</sub>)<sub>2</sub>Pz]H (0.468 g, 1.96 mmol) were mixed in a Schlenk flask charged with N<sub>2</sub> and toluene (25.0 mL) with 3 drops of acetonitrile. The resulting mixture was protected from light by wrapping with an aluminum foil and was refluxed overnight. After it

was cooled, the solution was filtered through a bed of Celite to remove insoluble unreacted silver oxide. The solvent in the filtrate collected was removed under reduced pressure to give  $\{[4\text{-Cl-}3,5-(\text{CF}_3)_2\text{Pz}]\text{Ag}\}_3$  as an off-white solid. Then the compound was further vacuum-dried at 100 °C for 6 h to remove all solvent, and X-ray quality crystals were grown from hexane at 5 °C. Yield: 88% (based on the amount of pyrazole used). Melting point 270–272 °C. <sup>19</sup>F NMR (CDCl<sub>3</sub>): δ -61.7 (s, CF<sub>3</sub>). <sup>13</sup>C NMR (CDCl<sub>3</sub>): δ 109.6 (s, 4-C), 118.7 (q, CF<sub>3</sub>, J<sub>C-F</sub> = 270.8 Hz), 141.7 (q, 3-C and 5-C, J<sub>C-F</sub> = 35.2 Hz) Anal. Calcd for C<sub>15</sub>Ag<sub>3</sub>N<sub>6</sub>F<sub>18</sub>Cl<sub>3</sub>: C, 17.39; N, 8.11. Found: C, 17.66; N, 8.52.

**Synthesis of  $\{[4\text{-Br-}3,5-(\text{CF}_3)_2\text{Pz}]\text{Ag}\}_3$ .** Ag<sub>2</sub>O (0.248 g, 1.07 mmol) and [4-Br-3,5-(CF<sub>3</sub>)<sub>2</sub>Pz]H (0.556 g, 1.92 mmol) were mixed in a Schlenk flask under N<sub>2</sub> and charged with 25.0 mL of toluene containing 3 drops of acetonitrile. The resulting mixture was protected from light by wrapping with an aluminum foil and was refluxed overnight. After being cooled to the RT, the solution was filtered through a bed of Celite to remove insoluble unreacted silver oxide. The solvent in the filtrate collected was removed under reduced pressure to give  $\{[4\text{-Br-}3,5-(\text{CF}_3)_2\text{Pz}]\text{Ag}\}_3$  as a white solid and further, the compound was vacuum-dried at 100 °C for 6 h. X-ray quality crystals were grown from dichloromethane at 5 °C. Yield: 94% (based on the amount of pyrazole used). Melting point 322–324 °C. <sup>19</sup>F NMR (CDCl<sub>3</sub>): δ -61.5 (s, CF<sub>3</sub>). <sup>13</sup>C NMR (DMSO): δ 90.3 (s, 4-C), 120.4 (q, CF<sub>3</sub>, J<sub>C-F</sub> = 270.4 Hz), 141.9 (q, 3-C and 5-C, J<sub>C-F</sub> = 36.5 Hz). Anal. Calcd for C<sub>15</sub>Ag<sub>3</sub>N<sub>6</sub>F<sub>18</sub>Br<sub>3</sub>: C, 15.40; N, 7.19. Found: C, 15.92; N, 7.47.

**X-ray Crystallographic Data.** A suitable crystal covered with a layer of hydrocarbon/paratone-N oil was selected and mounted on a Cryo-loop, and immediately placed in the low temperature nitrogen stream. The X-ray intensity data were measured at 100(2) K (except where indicated as noted below) on a Bruker SMART APEX CCD area detector system equipped with an Oxford Cryosystems 700 series cooler, a graphite monochromator, and a Mo K $\alpha$  fine-focus sealed tube ( $\lambda$  = 0.71073 Å). Intensity data were processed using the Saint Plus program. All the calculations for the structure determination were carried out using the SHELXTL package (version 6.14). Initial atomic positions were located by direct methods using XS, and the structures of the compounds were refined by the least-squares method using XL. Absorption corrections were applied by using SADABS. All atoms (compound contains no H-atoms) were refined anisotropically. Further details of the data collection and refinement are given in the Supporting Information as CIF files.

$\{[4\text{-Cl-}3,5-(\text{CF}_3)_2\text{Pz}]\text{Cu}\}_3$  crystallizes in the  $P\bar{1}$  space group with one molecule in the asymmetric unit (for a Z value of 2). Crystals cracked at low temperature (100 K); thus, data was collected at RT. As a result, many of the fluorine atoms had large thermal ellipsoids which resulted in several NPD messages during refinement. These were treated with ISOR restraints. Most of the  $\{[4\text{-Br-}3,5-(\text{CF}_3)_2\text{Pz}]\text{Cu}\}_3$  crystals were twinned and tend to crack at low temperature. Data was collected on a small crystal at RT and as a result completeness at the highest resolution is about 93%. Compound crystallizes in the  $P2_1/n$  space group with two independent molecules in the asymmetric unit (for a Z value of 8). Fluorine atoms from the CF<sub>3</sub> groups demonstrated rotational disorder and were treated with a combination of ISOR and FVAR instructions.  $\{[4\text{-Cl-}3,5-(\text{CF}_3)_2\text{Pz}]\text{Ag}\}_3$  crystallizes in the  $Pbca$  space group with one molecule in the asymmetric unit (for a Z value of 8). Two CF<sub>3</sub> groups demonstrate rotational disorder and were modeled and treated with FVAR instructions. Related  $\{[4\text{-Br-}3,5-(\text{CF}_3)_2\text{Pz}]\text{Ag}\}_3$  crystallizes in the  $Pbca$  space group with one molecule in the asymmetric unit (for a Z value of 8). Structure refined smoothly with no apparent issues.

## ASSOCIATED CONTENT

### Supporting Information

CIF and X-ray crystallographic data tables. This material is available free of charge via the Internet at <http://pubs.acs.org>.

## AUTHOR INFORMATION

## Corresponding Authors

\*E-mail: champikav@pdn.ac.lk (C.V.H.).

\*E-mail: momary@twu.edu (M.A.R.O.).

\*E-mail: dias@uta.edu (H.V.R.D.).

## Notes

The authors declare no competing financial interest.

## ACKNOWLEDGMENTS

This work was supported by the National Science Foundation (CHE-0845321 and CHE-1265807) and the Robert A. Welch Foundation (Grant Y-1289). C.V.H. is grateful to the Fulbright Foundation for awarding an Advanced Research and Lecturing Fellowship 2012–2013 to work at the University of Texas, Arlington. M.A.R.O. acknowledges support of her group contribution to a departmental research grant by the Robert A. Welch Foundation and a Texas Woman's University intramural REP grant. The X-ray crystallography was performed in the Center for Nanostructured Materials (CNM) at the University of Texas at Arlington. We thank Naleen Jayaratna for the technical support.

## REFERENCES

- (1) La Monica, G.; Ardizzoia, G. A. *Prog. Inorg. Chem.* **1997**, *46*, 151–238.
- (2) Zhang, J.-P.; Zhang, Y.-B.; Lin, J.-B.; Chen, X.-M. *Chem. Rev.* **2012**, *112*, 1001–1033.
- (3) Masciocchi, N.; Moret, M.; Cairati, P.; Sironi, A.; Ardizzoia, G. A.; La Monica, G. *J. Am. Chem. Soc.* **1994**, *116*, 7668–7676.
- (4) Murray, H. H.; Raptis, R. G.; Fackler, J. P., Jr. *Inorg. Chem.* **1988**, *27*, 26–33.
- (5) Kishimura, A.; Yamashita, T.; Yamaguchi, K.; Aida, T. *Nat. Mater.* **2005**, *4*, 546–549.
- (6) Kishimura, A.; Yamashita, T.; Aida, T. *J. Am. Chem. Soc.* **2005**, *127*, 179–183.
- (7) Lintang, H. O.; Kinbara, K.; Tanaka, K.; Yamashita, T.; Aida, T. *Angew. Chem., Int. Ed.* **2010**, *49*, 4241–4245.
- (8) Dias, H. V. R.; Diyabalanage, H. V. K.; Eldabaja, M. G.; Elbjairami, O.; Rawashdeh-Omary, M. A.; Omary, M. A. *J. Am. Chem. Soc.* **2005**, *127*, 7489–7501.
- (9) Jozak, T.; Sun, Y.; Schmitt, Y.; Lebedkin, S.; Kappes, M.; Gerhards, M.; Thiel, W. R. *Chem.—Eur. J.* **2011**, *17*, 3384–3389.
- (10) Barbera, J.; Lantero, I.; Moyano, S.; Serrano, J. L.; Elduque, A.; Gimenez, R. *Chem.—Eur. J.* **2011**, *16*, 14545–14553.
- (11) Rawashdeh-Omary, M. A. *Comments Inorg. Chem.* **2013**, *33*, 88–101.
- (12) Hou, L.; Shi, W.-J.; Wang, Y.-Y.; Wang, H.-H.; Cui, L.; Chen, P.-X.; Shi, Q.-Z. *Inorg. Chem.* **2011**, *50*, 261–270.
- (13) Singh, K.; Long, J. R.; Stavropoulos, P. *J. Am. Chem. Soc.* **1997**, *119*, 2942–2943.
- (14) Omary, M. A.; Rawashdeh-Omary, M. A.; Gonser, M. W. A.; Elbjairami, O.; Grimes, T.; Cundari, T. R.; Diyabalanage, H. V. K.; Gamage, C. S. P.; Dias, H. V. R. *Inorg. Chem.* **2005**, *44*, 8200–8210.
- (15) Scheele, U. J.; Georgiou, M.; John, M.; Dechert, S.; Meyer, F. *Organometallics* **2008**, *27*, 5146–5151.
- (16) Yang, G.; Raptis, R. G. *Inorg. Chim. Acta* **2007**, *360*, 2503–2506.
- (17) Dias, H. V. R.; Gamage, C. S. P.; Keltner, J.; Diyabalanage, H. V. K.; Omari, I.; Eyobo, Y.; Dias, N. R.; Roehr, N.; McKinney, L.; Poth, T. *Inorg. Chem.* **2007**, *46*, 2979–2987.
- (18) Mohamed, A. A.; Burini, A.; Fackler, J. P., Jr. *J. Am. Chem. Soc.* **2005**, *127*, 5012–5013.
- (19) Jahnke, A. C.; Proepper, K.; Bronner, C.; Teichgraber, J.; Dechert, S.; John, M.; Wenger, O. S.; Meyer, F. *J. Am. Chem. Soc.* **2012**, *134*, 2938–2941.
- (20) Titov, A. A.; Filippov, O. A.; Bilyachenko, A. N.; Smol'yakov, A. F.; Dolgushin, F. M.; Belsky, V. K.; Godovikov, I. A.; Epstein, L. M.; Shubina, E. S. *Eur. J. Inorg. Chem.* **2012**, 5554–5561.
- (21) Tekarli, S. M.; Cundari, T. R.; Omary, M. A. *J. Am. Chem. Soc.* **2008**, *130*, 1669–1675.
- (22) Burini, A.; Mohamed, A. A.; Fackler, J. P. *Comments Inorg. Chem.* **2003**, *24*, 253–280.
- (23) Yang, G.; Baran, P.; Martinez, A. R.; Raptis, R. G. *Cryst. Growth Des.* **2013**, *13*, 264–269.
- (24) Tsupreva, V. N.; Titov, A. A.; Filippov, O. A.; Bilyachenko, A. N.; Smol'yakov, A. F.; Dolgushin, F. M.; Agapkin, D. V.; Godovikov, I. A.; Epstein, L. M.; Shubina, E. S. *Inorg. Chem.* **2011**, *50*, 3325–3331.
- (25) Mohamed, A. A.; Galassi, R.; Papa, F.; Burini, A.; Fackler, J. P., Jr. *Inorg. Chem.* **2006**, *45*, 7770–7776.
- (26) Zhan, S.-Z.; Li, M.; Zhou, X.-P.; Li, D.; Ng, S. W. *RSC Adv.* **2011**, *1*, 1457–1459.
- (27) Krishantha, D. M. M.; Gamage, C. S. P.; Schelly, Z. A.; Dias, H. V. R. *Inorg. Chem.* **2008**, *47*, 7065–7067.
- (28) den Boer, D.; Krikorian, M.; Esser, B.; Swager, T. M. *J. Phys. Chem. C* **2013**, *117*, 8290–8298.
- (29) Dias, H. V. R.; Polach, S. A.; Wang, Z. *J. Fluorine Chem.* **2000**, *103*, 163–169.
- (30) Dias, H. V. R.; Diyabalanage, H. V. K.; Rawashdeh-Omary, M. A.; Franzman, M. A.; Omary, M. A. *J. Am. Chem. Soc.* **2003**, *125*, 12072–12073.
- (31) Omary, M. A.; Rawashdeh-Omary, M. A.; Diyabalanage, H. V. K.; Dias, H. V. R. *Inorg. Chem.* **2003**, *42*, 8612–8614.
- (32) Dias, H. V. R.; Diyabalanage, H. V. K.; Gamage, C. S. P. *Chem. Commun.* **2005**, 1619–1621.
- (33) Dias, H. V. R.; Diyabalanage, H. V. K. *Polyhedron* **2006**, *25*, 1655–1661.
- (34) Grimes, T.; Omary, M. A.; Dias, H. V. R.; Cundari, T. R. *J. Phys. Chem. A* **2006**, *110*, 5823–5830.
- (35) Dias, H. V. R.; Palehepitiya Gamage, C. S. *Angew. Chem., Int. Ed.* **2007**, *46*, 2192–2194.
- (36) Omary, M. A.; Elbjairami, O.; Gamage, C. S. P.; Sherman, K. M.; Dias, H. V. R. *Inorg. Chem.* **2009**, *48*, 1784–1786.
- (37) Rawashdeh-Omary, M. A.; Rashdan, M. D.; Dharanipathi, S.; Elbjairami, O.; Ramesh, P.; Dias, H. V. R. *Chem. Commun.* **2011**, *47*, 1160–1162.
- (38) Dias, H. V. R.; Singh, S.; Campana, C. F. *Inorg. Chem.* **2008**, *47*, 3943–3945.
- (39) Chi, Y.; Lay, E.; Chou, T.-Y.; Song, Y.-H.; Carty, A. J. *Chem. Vap. Deposition* **2005**, *11*, 206–212.
- (40) Vorontsov, I. I.; Kovalevsky, A. Y.; Chen, Y.-S.; Graber, T.; Gembicky, M.; Novozhilova, I. V.; Omary, M. A.; Coppens, P. *Phys. Rev. Lett.* **2005**, *94*, 193003/1–193003/4.
- (41) Banditelli, G.; Bandini, A. L.; Bonati, F.; Goel, R. G.; Minghetti, G. *Gazz. Chim. Ital.* **1982**, *112*, 539–542.
- (42) Maspero, A.; Giovenzana, G. B.; Monticelli, D.; Tagliapietra, S.; Palmisano, G.; Penoni, A. *J. Fluorine Chem.* **2012**, *139*, 53–57.
- (43) Bondi, A. J. *Phys. Chem. A* **1964**, *68*, 441–451.
- (44) Alvarez, S. *Dalton Trans.* **2013**, *42*, 8617–8636.
- (45) Batsanov, S. S. *Inorg. Mater.* **2001**, *37*, 871–885.
- (46) According to Batsanov (ref 45) van der Waals contact distances between Cu-Cl, Cu-Br, Ag-Cl, and Ag-Br are 3.8, 3.9, 3.9, and 4.0 Å, respectively. The corresponding van der Waals contact distances estimated by Alvarez (ref 44) are 4.20, 4.24, 4.35, 4.39 Å, respectively. Overall, based on these values, some of the observed M...Cl and M...Br separations may represent significant contacts.
- (47) Dance, I. *New J. Chem.* **2003**, *27*, 22–27.
- (48) Pyykko, P.; Runeberg, N.; Mendizabal, F. *Chem.—Eur. J.* **1997**, *3*, 1451–1457.
- (49) Butsanov and Alvarez (see refs 45 and 44, respectively) place van der Waals radius of copper at 2.0 and 2.38 Å (thus Cu-Cu van der Waals contact radii at 4.0 and 4.76 Å), and silver at 2.1 and 2.53 Å (corresponding Ag-Ag van der Waals contact distances at 4.2 and 5.06 Å), respectively.